

## Electronic Supplementary Information (ESI) for:

### Micro-/Nano-Sized Multifunctional Heterochiral Metal-Organic Frameworks for High-Performance Visible-Blind UV Photodetectors

Xiaobo Shang,<sup>‡ab</sup> Inho Song,<sup>‡a</sup> Gwan Yeong Jung,<sup>c</sup> Wanuk Choi,<sup>d</sup> Hiroyoshi Ohtsu,<sup>e</sup> Jeong Hyeon Lee,<sup>c</sup> Jaeyong Ahn,<sup>a</sup> Jin Young Koo,<sup>f</sup> Masaki Kawano,<sup>e</sup> Sang Kyu Kwak,<sup>d</sup> and Joon Hak Oh<sup>\*a</sup>

<sup>a</sup>School of Chemical and Biological Engineering, Institute of Chemical Processes, Seoul National University, 1 Gwanak-ro, Gwanak-gu, Seoul 08826, South Korea  
E-mail: joonhoh@snu.ac.kr

<sup>b</sup>Department of Polymer Science and Engineering, Zhejiang University, Hangzhou 310027, China

<sup>c</sup>Department of Energy Engineering, School of Energy and Chemical Engineering, Ulsan National Institute of Science and Technology (UNIST), Ulsan 44919, South Korea

<sup>d</sup>Energy Materials Laboratory, Korea Institute of Energy Research (KIER), Daejeon, 34129, South Korea

<sup>e</sup>Department of Chemistry, School of Science, Tokyo Institute of Technology, 2-12-1 Ookayama, Meguro-ku, Tokyo 152-8550, Japan

<sup>f</sup>Department of Chemistry, Pohang University of Science and Technology (POSTECH), Pohang, Gyeongbuk 37673, South Korea

<sup>‡</sup>Xiaobo Shang and Inho Song equally contributed to this work.

## Supplementary Contents

Estimation of electrical conductivity and optoelectronic parameters ----- S3

## Supplementary Figures

TGA curves of homochiral and heterochiral AlaNDI-Ca MOFs (Fig. S1) ----- S5

SEM images of heterochiral AlaNDI-Ca MOFs (Fig. S2) ----- S6

PXRD results of heterochiral AlaNDI-Ca MOFs (Fig. S3) ----- S7

IR results of heterochiral AlaNDI-Ca MOFs (Fig. S4) ----- S8

ESR results of homochiral AlaNDI-Ca MOFs (Fig. S5) ----- S9

Time-dependent conductivity changes of heterochiral AlaNDI-Ca MOFs (Fig. S6) ----- S10

## Estimation of electrical conductivity and optoelectronic parameters

The electrical conductivity of MOFs was calculated from two-probe method using the following equation:

$$\sigma = G \frac{l}{A} = \frac{I}{V} \times \frac{l}{A} \quad (\text{S1})$$

where  $G$  is electrical conductance, and  $l$  and  $A$  are length and area of the conduction channel, respectively. The length and area of the conduction channel were measured using the SEM image of AlaNDI-Ca micro-/nanocrystals.

To investigate the possible optoelectronic applications of our heterochiral AlaNDI-Ca MOFs micro-/nanocrystals, the  $R$  and  $P$  values were calculated from  $I$ - $V$  curves before and after UV light irradiation. These are typically defined by the following equations:

$$R = \frac{I_{\text{ph}}}{P_{\text{inc}}} = \frac{I_{\text{light}} - I_{\text{dark}}}{P_{\text{inc}}} \quad (\text{S2})$$

$$P = \frac{I_{\text{light}} - I_{\text{dark}}}{I_{\text{dark}}} \quad (\text{S3})$$

where  $I_{\text{ph}}$  is the photocurrent,  $P_{\text{inc}}$  is the incident illumination power on the channel of the device,  $I_{\text{light}}$  is the current under illumination, and  $I_{\text{dark}}$  is the current in the dark.

In addition, the EQE of these resistor-type photodetectors, defined as the ratio of the number of photogenerated carriers to the number of photons incident on the photodetector channel area, was calculated using the following equation:

$$\eta = \frac{(I_{\text{light}} - I_{\text{dark}})hc}{eP_{\text{int}}A\lambda_{\text{peak}}} \quad (\text{S4})$$

where  $h$  is Plank's constant,  $c$  is the speed of light,  $e$  is the fundamental unit of charge,  $P_{\text{int}}$  the incident power density,  $A$  is the area of the detector channel, and  $\lambda_{\text{peak}}$  is the peak wavelength of the incident light, respectively. The channel area was confirmed from the optical microscope

images of individual MOF crystals. The  $\lambda_{\text{peak}}$  of the illuminated light source was 365 nm and the incident optical power density was  $150 \mu\text{W cm}^{-2}$ .

Furthermore,  $D^*$  is an important figure of merit for photodetectors.  $D^*$  describes the smallest detectable signal and allows for comparison between photodetector devices with different configurations and active areas.  $D^*$  is estimated for our heterochiral MOF-based photodetectors using the following equations:

$$D^* = \frac{\sqrt{A}}{NEP} \quad (\text{S5})$$

$$NEP = \frac{\sqrt{\overline{I_n^2}}}{R} \quad (\text{S6})$$

where  $A$  is the active area of the photodetector,  $NEP$  is the noise equivalent power, and  $\overline{I_n^2}$  is the measured noise current. If shot noise from the dark current is the major contributor to the noise that limits detectivity, then  $D^*$  can be simplified to:

$$D^* = \frac{R}{\sqrt{(2e \cdot I_{\text{dark}}/A)}} \quad (\text{S7})$$

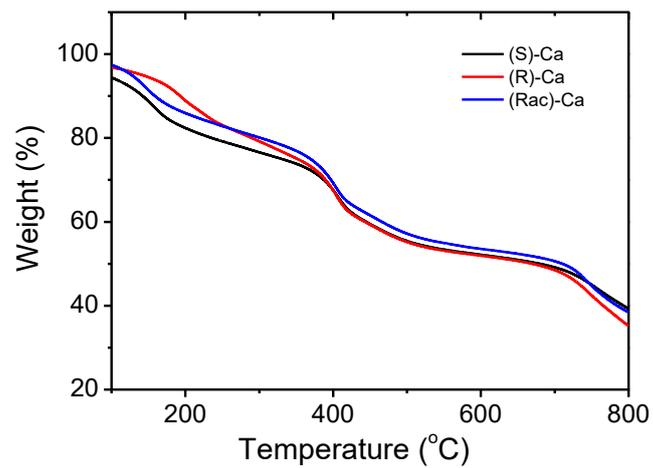
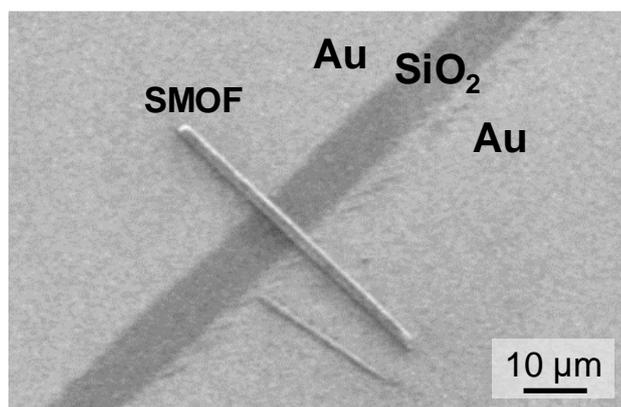


**Fig. S1** TGA curves of homochiral and heterochiral Al<sub>3</sub>NDI-Ca MOFs.



**Fig, S2** SEM images of (*Rac*)-AlaNDI-Ca MOFs on pre-patterned gold electrodes in electronic devices.

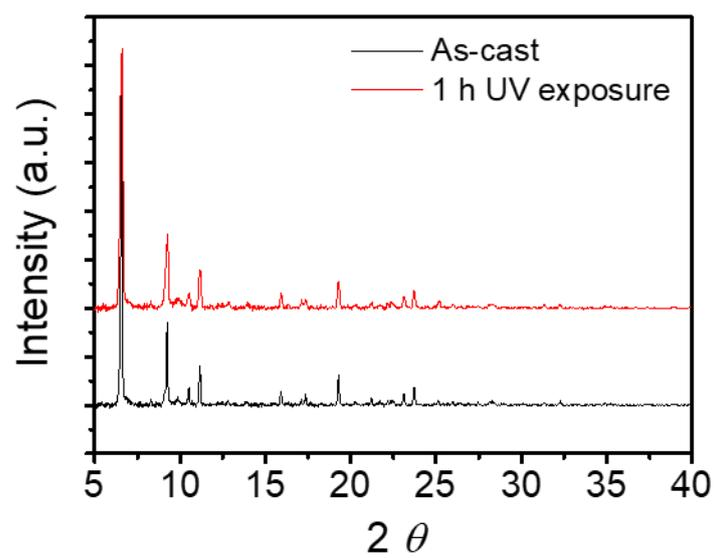


**Fig. S3** PXRD results of heterochiral AlaNDI-Ca MOFs before and after exposure to UV light ( $\lambda = 365$  nm,  $150 \mu\text{W cm}^{-2}$ ) for 1 h.

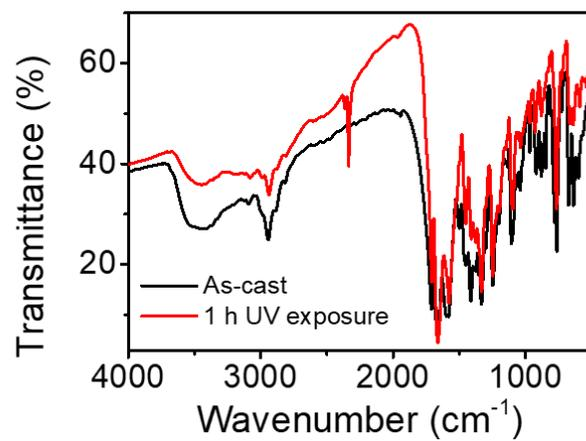


**Fig. S4** IR results of heterochiral AlaNDI-Ca MOFs before and after exposure of UV light ( $\lambda = 365$  nm,  $150 \mu\text{W cm}^{-2}$ ) for 1 h.

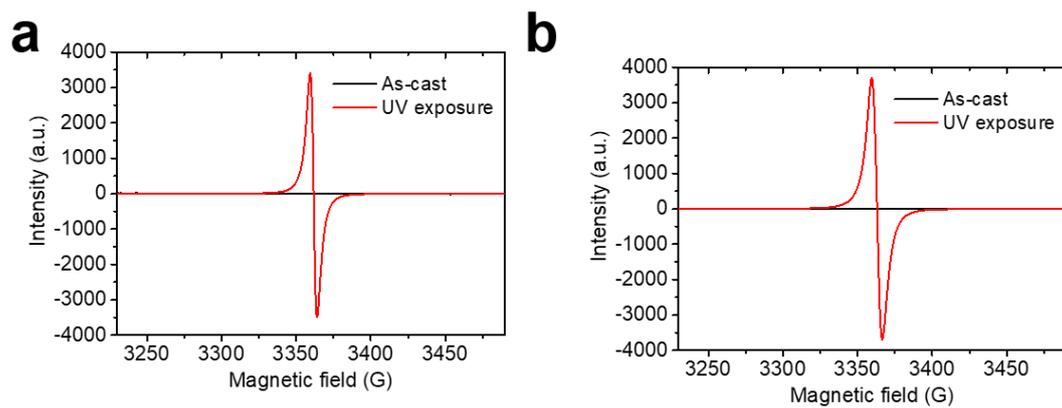


**Fig. S5** ESR results of homochiral (a) (*R*)- and (b) (*S*)-AlaNDI-Ca MOFs before and after exposure to UV light ( $\lambda = 365$  nm,  $150 \mu\text{W cm}^{-2}$ ) for 1 h.

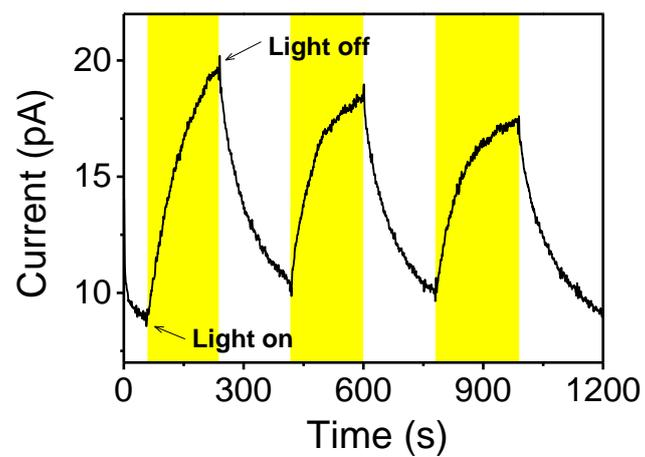


**Fig. S6** Time-dependent conductivity changes of heterochiral (*Rac*)-AlaNDI-Ca MOFs under UV light ( $\lambda = 365$  nm,  $150 \mu\text{W cm}^{-2}$ ) for repetitive photoswitching test.